

## Green, yellow, and orange defect emission from ZnO nanostructures: Influence of excitation wavelength

A. B. Djurišić,<sup>a)</sup> Y. H. Leung, and K. H. Tam

*Department of Physics, The University of Hong Kong, Pokfulam Road, Hong Kong*

L. Ding and W. K. Ge

*Department of Physics, The Hong Kong University of Science and Technology, Clear Water Bay, Hong Kong*

H. Y. Chen and S. Gwo

*Department of Physics, National Tsing Hua University, 101, Sec. 2, Huang-Fu Road, Hsinchu 300, Taiwan*

(Received 26 October 2005; accepted 8 January 2006; published online 7 March 2006)

ZnO commonly exhibits luminescence in the visible spectral range due to different intrinsic defects. In order to study defect emissions, photoluminescence from ZnO nanostructures prepared by different methods (needles, rods, shells) was measured as a function of excitation wavelength and temperature. Under excitation at 325 nm, needles exhibited orange-red defect emission, rods exhibited yellow defect emission, while shells exhibited green defect emission. Obvious color change from orange to green was observed for needles with increasing excitation wavelengths, while nanorods (yellow) showed smaller wavelength shift and shells (green) showed no significant spectral shift. Reasons for different wavelength dependences are discussed. © 2006 American Institute of Physics. [DOI: 10.1063/1.2182096]

ZnO is a wide band gap semiconductor with high excitation binding energy (60 meV), so that there is intense interest in studying its optical properties.<sup>1–23</sup> In addition to UV excitonic emission peak, ZnO commonly exhibits visible luminescence at different emission wavelengths due to intrinsic or extrinsic defects.<sup>1</sup> The origin of these emissions, especially the green emission, has been controversial.<sup>1</sup> A number of different hypotheses have been proposed to explain the green emission, such as transition between singly ionized oxygen vacancy and photoexcited hole,<sup>21</sup> transition between electron close to the conduction band and a deeply trapped hole at  $V_o^{++}$ ,<sup>22</sup> surface defects,<sup>1</sup> etc. While green emission is typically associated with oxygen deficiency, yellow/orange emission is associated with excess oxygen.<sup>5</sup> The yellow-orange defect emission observed in ZnO synthesized by a hydrothermal method is typically assigned to interstitial oxygen,<sup>2,19</sup> although other hypotheses such as dislocation related luminescence centers<sup>8</sup> and Li dopants<sup>16</sup> have been proposed. The assignment of the emission to interstitial oxygen has been confirmed by reduction of this emission after annealing in a reducing environment.<sup>19</sup> Unlike green emission, yellow emission is not significantly influenced by the surface modifications.<sup>2</sup> On the other hand, red-orange emission (peak position at ~640–680 nm or ~1.8–1.9 eV) has been less commonly observed than green and yellow emissions.<sup>5–10</sup>

These three emissions (green at ~2.3 eV, yellow at ~2.1 eV, and red at ~1.8 eV) were assigned to three different types of defects based on depth resolved cathodoluminescence and PL measurements.<sup>20</sup> Distinctly different origin of the yellow emission compared to red/near IR emission was also confirmed in nitrogen doped ZnO based on their different behavior with electron bombardment,<sup>6</sup> as well as ZnO single crystals based on time resolved luminescence.<sup>13</sup> The near IR emission at 1.70 eV and yellow emission at

~2.02 eV were found to have different decay properties, and it was proposed that they involve similar final states but different initial states (conduction band and donor centers).<sup>13</sup> However, there have been contradictory reports on the observations of green and orange emissions. Lack of simultaneous observation of green and orange-red emissions was reported.<sup>5,9</sup> Orange emission (640 nm) in ZnO nanorods was found to coexist with the blue emission (468 nm), and it was enhanced by annealing in air, while annealing in ammonia resulted in disappearance of orange and appearance of green (510 nm) emission.<sup>9</sup> However, other studies report the coexistence of green (~520 nm) and red (~672 nm) emissions in ZnO films<sup>10</sup> and ZnO single crystals, where different spatiotemporal behavior of green and orange-red emission was found.<sup>12</sup> The proposed explanation of this emission was a transition between neutral and singly ionized oxygen vacancy,<sup>10</sup> contradicting studies which associated orange-red emission with excess oxygen.<sup>5,9</sup>

Assignment of various defect emissions to the specific transitions in ZnO is often complicated by the presence of multiple emissions and broad emission peaks containing contributions from multiple transitions. In order to study the luminescence from defects responsible for green, yellow, and orange emissions, we prepared nanostructures exhibiting different defect emissions when excited by a He–Cd laser at 325 nm. The needles,<sup>2</sup> rods,<sup>3</sup> and hollow shells<sup>4</sup> were prepared according to previously reported procedures. It is well known that defect types and concentrations, as well as nanostructure morphology, are determined by fabrication conditions (pressure, temperature, flow rate, etc.). Different fabrication methods resulted in different morphologies, as well as different defect types and concentrations resulting in different luminescence spectra. These three types of nanostructures have been chosen since they exhibit clear dominance of one type of defect emission under 325 nm excitation. Since the same defect emissions (green, yellow, and orange-red)

<sup>a)</sup>Electronic mail: dalek@hkusua.hku.hk

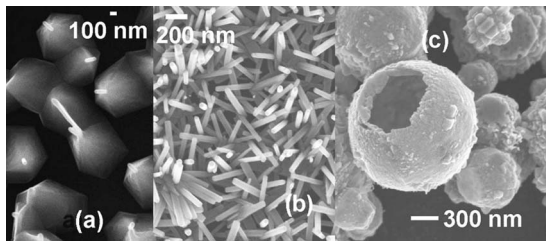


FIG. 1. Representative SEM images of the nanostructures studied: (a) needles, (b) rods, and (c) shells.

can be observed in ZnO with various morphologies, it is reasonable to assume that they are not dependent on morphology but rather on dominant defect type. The morphology of the nanostructures was examined by scanning electron microscopy (SEM) using a Leo 1530 field emission SEM. For variable temperature photoluminescence measurements, samples were mounted at the cold finger and placed in a closed-cycle He cryostat (APD Cryogenics, Inc. model HC-2). The excitation sources were a HeCd laser for 325 nm and a frequency doubled Ti:sapphire pulsed laser for 380, 390, and 400 nm. The spectra were dispersed by a spectrometer SPEX 500M and recorded by a photomultiplier tube R943.

Figure 1 shows the representative SEM images of the investigated nanostructures. All the measurements were performed over ensembles of nanostructures with densities of individual nanostructures per laser spot area of several hundred for shells and needles and several thousand for rods. Thus, observed intensity represents an average over a large number of nanostructures. The nanorod diameter is in the range 30–50 nm, the shell diameter is in the range 300 nm–2  $\mu$ m, while the needles consist of very thin (20–60 nm) rods on top of a wider base. For this size range, no quantum size effects are expected to be observed in ZnO. However, different surface to volume ratios of nanostructures with different diameters may affect the intensities of the defect emissions, but the difference in peak positions is not expected to be significant.

Photoluminescence spectra from shells, rods, and needles were measured for different excitation wavelengths (325, 380, 390, and 400 nm). Obtained results are shown in Figs. 2(a)–2(c). In all cases, the emission intensity decreases with increasing excitation wavelength, as expected. However, the significantly different behavior is observed for the peak position. While the emission from the needles is orange for excitation at 325 and 380 nm, it becomes green for 390 and 400 nm. The emission from rods is also blueshifted with increasing excitation wavelength, although the shift is less significant compared to the needles. On the other hand, green emission from the shells did not exhibit significant position changes with increasing excitation wavelength. Since green emission can only be excited above 380 nm and orange emission can only be excited above 380 nm and orange emission can only be excited for excitation wavelengths  $\lambda \leq 380$  nm, it is possible that the observed shift of the yellow emission from rod samples with increasing excitation wavelength is due to the disappearance of the orange component of the emission. Different defect emissions also exhibited different temperature dependences, as shown in Fig. 3(a), and different changes upon annealing at 600 °C in air, as shown in Fig. 3(b). It can be observed that all the peak positions either exhibit no change or show small blueshift with increasing temperature. In the case of needles for 390 nm

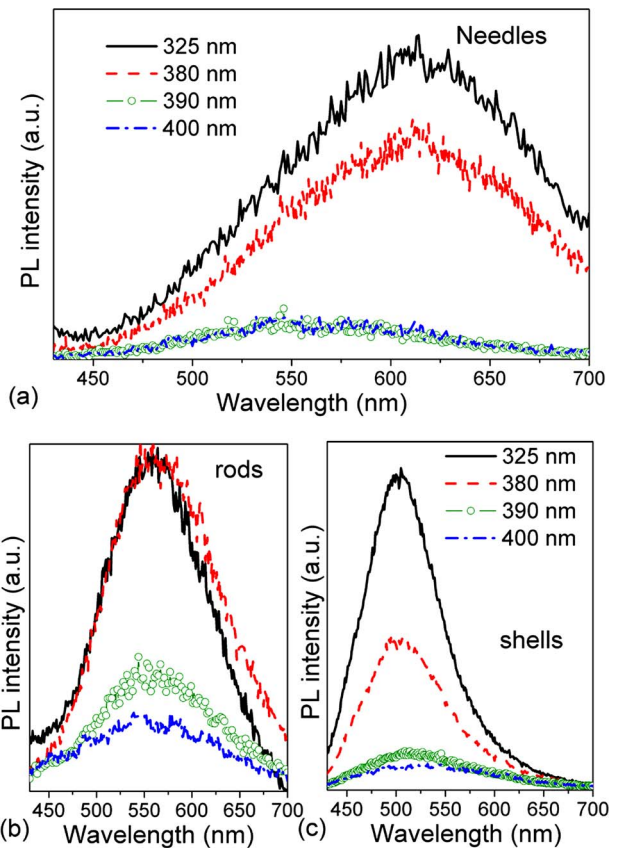


FIG. 2. (Color online) Room temperature PL spectra for different excitation wavelengths (a) needles, (b) rods, and (c) shells.

excitation at low temperature blue defect emission can also be observed. Blue emission (466–468 nm), coexistent with yellow-orange emission (612–640 nm), was previously observed in ZnO,<sup>9,23</sup> but the origin of this emission was not fully clear.

While there are numerous studies of the PL spectra of ZnO, photoluminescence excitation (PLE) measurements<sup>11,13,15</sup> or the studies of PL with variable excitation wavelength have been scarce and reported results have been contradictory. It was reported that yellow (2.02 eV) and near IR (1.70 eV) are excited at band edge and lower ener-

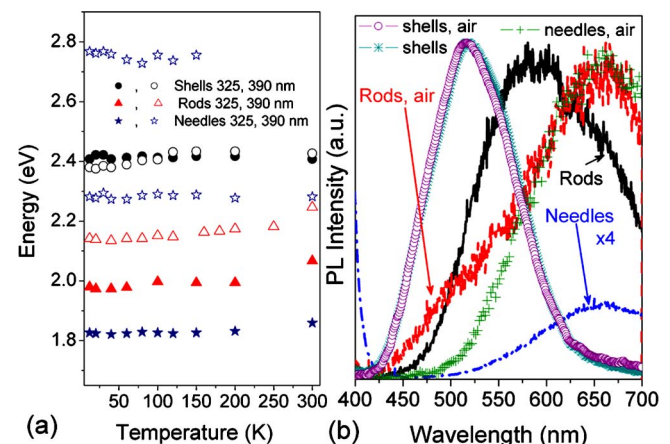


FIG. 3. (Color online) (a) Defect emission peak positions vs temperature for different excitation wavelengths (325 and 390 nm) and different nanostructures (needles, rods, and shells) and (b) changes in the emission spectra after annealing in air at 600 °C for 30 min. “Air” in the label after morphology description (e.g., shells, air) indicates annealed samples.

gies, while green emission (2.44 eV) could be excited only at the band edge.<sup>13</sup> These results contradict other PLE reports<sup>11,15</sup> and our observation that green and yellow luminescence could be excited above 380 nm, while the opposite is the case for orange-red emission. PLE results of Gaspar *et al.*<sup>15</sup> indicate that green and yellow emission have the same onset at  $\sim 3.00$  eV, in agreement with our results. On the other hand, Lima *et al.*<sup>11</sup> reported that both red and green luminescence could be excited below the band edge. One possible reason for the discrepancies between different PLE reports in the literature is the large spectral width of the defect emissions. When the sample contains both yellow and orange-red emissions, it is very difficult to distinguish which of the two defect levels can be excited at different excitation wavelengths. For example, our nanorod samples exhibit strong and broad yellow defect emission. This emission consists of a small green component, which is likely due to surface defects,<sup>3</sup> and dominant broad yellow emission, whose width makes it difficult to resolve components in red (640–700 nm) spectral range. On the other hand, needles do not have a strong yellow component of the emission and enable us to study the orange-red emission independently from the yellow one. The fact that both emissions are reduced by annealing in argon indicates that both emissions are likely related to excess oxygen. However, annealing in air considerably enhances orange-red emission and not yellow, while green emission is not significantly changed, as shown in Fig. 3(b).

Thus, our results indicate that green, yellow, and orange-red emissions likely originate from different defect-related transitions, in agreement with the literature.<sup>5,6,9,13,20</sup> Due to the absence of redshift of the defect emission with increasing temperature, it is likely that the observed emissions are not due to the direct transition between the electron in the conduction band and the deep level.<sup>15</sup> Thus, one possible explanation is that green and yellow emissions involve transitions from shallow donor to deep acceptor level, and that two different acceptor defects are involved. On the other hand, orange-red emission could only be excited at or above the band edge. This indicates that the orange emission involves recombination centers with large Stokes shift with their excited states being resonant with the conduction band. The energy level calculations for ZnO<sup>11,24</sup> reveal several possible candidates for these defect levels and their exact identification requires further study.

To summarize, we have measured photoluminescence of different ZnO nanostructures exhibiting green, yellow, and orange-red defect emissions as a function of excitation wave-

length and the temperature. It was found that the green and yellow emission could be excited by excitation below the band edge, while the orange-red emission could be excited only by excitation above the band edge. Consequently, the defect emission from needles changed from orange-red to green luminescence when excitation wavelength changed from 325 to 390 nm.

This work is partly supported by the Research Grant Council of the Hong Kong Special Administrative Region, China (Grant No. HKU 7019/04P) and University Development Fund grant of the University of Hong Kong.

<sup>1</sup>A. B. Djurišić, W. C. H. Choy, V. A. L. Roy, Y. H. Leung, C. Y. Kwong, K. W. Cheah, T. K. Gundu Rao, W. K. Chan, H. F. Lui, and C. Surya, *Adv. Funct. Mater.* **14**, 856 (2004).

<sup>2</sup>W. M. Kwok, Y. H. Leung, A. B. Djurišić, W. K. Chan, and D. L. Phillips, *Appl. Phys. Lett.* **87**, 093108 (2005).

<sup>3</sup>D. Li, Y. H. Leung, A. B. Djurišić, Z. T. Liu, M. H. Xie, S. L. Shi, S. J. Xu, and W. K. Chan, *Appl. Phys. Lett.* **85**, 1601 (2004).

<sup>4</sup>Y. H. Leung, K. H. Tam, A. B. Djurišić, M. H. Xie, W. K. Chan, Ding Lu, and W. K. Ge, *J. Cryst. Growth* **283**, 134 (2005).

<sup>5</sup>S. A. Studenikin, N. Golego, and M. Cocivera, *J. Appl. Phys.* **84**, 2287 (1998).

<sup>6</sup>Y. F. Mei, G. G. Siu, R. K. Y. Fu, K. W. Wong, P. K. Chu, C. W. Lai, and H. C. Ong, *Nucl. Instrum. Methods Phys. Res. B* **237**, 307 (2005).

<sup>7</sup>L. S. Vlasenko, and G. D. Watkins, *Phys. Rev. B* **72**, 035203 (2005).

<sup>8</sup>R. Radoi, P. Fernández, J. Piqueras, M. S. Wiggins, and J. Solis, *Nanotechnology* **14**, 794 (2003).

<sup>9</sup>L. Wu, Y. Wu, X. Pan, and F. Kong, *Opt. Mater.* **28**, 418 (2006).

<sup>10</sup>A. El Hichou, M. Addou, J. Ebothé, and M. Troyon, *J. Lumin.* **113**, 183 (2005).

<sup>11</sup>S. A. M. Lima, F. A. Sigoli, M. Jafellicci, Jr., and M. R. Davolos, *Int. J. Inorg. Mater.* **3**, 749 (2001).

<sup>12</sup>H. Priller, M. Decker, R. Hauschild, H. Kalt, and C. Klingshirn, *Appl. Phys. Lett.* **86**, 111909 (2005).

<sup>13</sup>R. B. Lauer, *J. Phys. Chem. Solids* **34**, 249 (1973).

<sup>14</sup>T. Minami, H. Nanto, and S. Takata, *J. Lumin.* **24/25**, 63 (1981).

<sup>15</sup>C. Gaspar, F. Costa, and T. Monteiro, *J. Mater. Sci.: Mater. Electron.* **12**, 269 (2001).

<sup>16</sup>N. Ohashi, N. Ebisawa, T. Sekiguchi, I. Sakaguchi, Y. Wada, T. Takenaka, and H. Haneda, *Appl. Phys. Lett.* **86**, 091902 (2005).

<sup>17</sup>T. Sekiguchi, S. Miyashita, K. Obara, T. Shishido, and N. Sakagami, *J. Cryst. Growth* **214/215**, 72 (2000).

<sup>18</sup>Yu. V. Gorkinskii and G. D. Watkins, *Phys. Rev. B* **69**, 115212 (2004).

<sup>19</sup>L. E. Greene, M. Law, J. Goldberger, F. Kim, J. C. Johnson, Y. Zhang, R. J. Saykally, and P. Yang, *Angew. Chem., Int. Ed.* **42**, 3031 (2003).

<sup>20</sup>H. C. Ong, and G. T. Du, *J. Cryst. Growth* **265**, 471 (2004).

<sup>21</sup>K. Vanheusden, C. H. Seager, W. L. Warren, D. R. Tallant, and J. A. Voigt, *Appl. Phys. Lett.* **68**, 403 (1996).

<sup>22</sup>A. van Dijken, E. A. Meulenkaamp, D. Vanmaekelbergh, and A. Meijerink, *J. Phys. Chem. B* **104**, 1715 (2000).

<sup>23</sup>L. Dai, X. L. Chen, W. J. Wang, T. Zhou, and B. Q. Hu, *J. Phys.: Condens. Matter* **15**, 2221 (2003).

<sup>24</sup>P. S. Xu, Y. M. Sun, C. S. Shi, F. Q. Xu, and H. B. Pan, *Nucl. Instrum. Methods Phys. Res. B* **199**, 286 (2003).